ARTICLES

Electrohydrodynamic stability of a liquid column under cross fields: Application to continuous flow electrophoresis

L. Limat
Laboratoire de Physique et de Mécanique des Milieux Hétérogènes, URA CNRS 857, ESPCI, 10 rue Vauquelin, 75005 Paris, France

H. A. Stone
Division of Engineering and Applied Sciences, Harvard University, Cambridge, Massachusetts 02138

J. L. Viovy
Laboratoire de Physico-Chimie Théorique, ESPCI, 10 rue Vauquelin, URA CNRS 1382, 75005 Paris, France

(Received 10 January 1997; accepted 17 June 1998)

An infinite, conductive cylindrical column of electrolyte lying inside another electrolyte flattens when it is submitted to a transverse continuous electric field. This ''ribbon'' effect can be canceled by a second oscillatory field whose direction is perpendicular to both the column axis and to the first electric field. The linear stability of the equilibrium with respect to elliptic perturbations of the cross section is studied, and it is shown that the stability of the circular shape depends on the sign of a discriminating function of the conductivity and permittivity ratios. Possible applications of the results to continuous flow electrophoresis are discussed: Even for unstable situations the growth rate of disturbances is reduced by the application of a second field so that we expect the efficiency of the separation to be improved. © *1998 American Institute of Physics.* [S1070-6631(98)01210-0]

I. INTRODUCTION

Electrohydrodynamic effects and flows[1] are of central importance in many problems of colloidal hydrodynamics,[2] especially for the separation of charged particles, as occurs during electrophoresis of colloids, proteins, DNA, cells and many other particles of biological interest.[3–9] These flows may also play an essential role in diverse biological processes, such as cell motility[10] or the natural function of ''biological motors.'' [11] In the present article, we consider the electrohydrodynamic flows encountered in the preparative separation method called continuous flow electrophoresis (CFE).[5–9] This method involves no interaction of the particles to be separated with a solid medium (e.g., as in gel electrophoresis or chromatography), so that it offers important potential advantages for the purification of fragile compounds, such as native proteins or cells.

The principle of the method can be summarized as follows: a laminar flow of an electrolyte is established in an elongated parallelepipedic chamber (Fig. 1). The flow direction is parallel to the chamber's long axis, which is typically of the order of a few tens of centimeters. A stream of the solution, containing the sample to be separated, is continuously introduced in the chamber, close to the inlet of the supporting electrolyte. A continuous electric field is applied along the width of the chamber (generally by means of two electrodes separated from the separation chamber by ion-permeable membranes), perpendicular to the flow direction. The components of the sample that have different electrophoretic mobilities move under the combined action of the flow and of their electrophoretic migration, and separate into different streams of purified products (Fig. 1).

These products are continuously collected in different channels at the end of the separation chamber. Both fluids are miscible, so surface tension is not important, and the residence time in the chamber is chosen low enough to avoid significant distortion of the sample stream by diffusion. Ideally, then, all streams of purified products should retain the initial (circular) cross section of the sample stream, and the final resolution of this separation process should depend on the width of this stream, on the differences in electrophoretic velocities, and the residence time in the chamber. However, several adverse effects tend to distort the laminar flow of the sample and products stream, thereby altering the resolution, and reducing these adverse effects is a key to practical applications of the separation method. Such effects are sedimentation, thermal convection and electro-osmosis.[6]

Combined with the action of the Poiseuille flow profile established in the rectangular chamber, these adverse effects lead to a typical ''crescent'' shape of the filament cross section that prevents satisfactory separation. When these deformations are minimized by an optimization of the cell geometry and the experimental conditions (and perhaps the use of microgravity), an electrohydrodynamic distortion due to the difference of conductivity or permittivity between the two fluids remains. This effect, first discussed by Rhodes *et al.*,[5] leads to a flattening of the filament into a ribbon, that ultimately evolves towards the ''crescent'' shape. The flattening

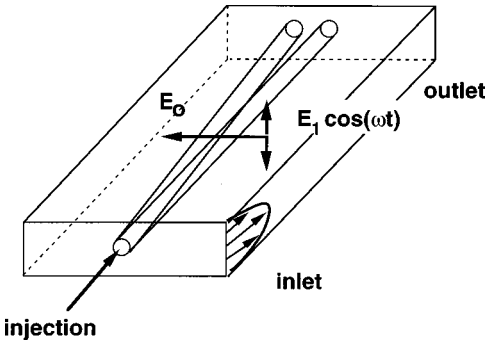

FIG. 1. Schematic view of a CFE (continuous flow electrophoresis) chamber.

direction depends on the sign of a discriminating function of the conductivity ratio $R=\mu_i/\mu_e$, and of the electric permittivity ratio $S=K_i/K_e$

$$D_f=R^2+R+1-3S, \tag{1}$$

where subscripts i and e denote the internal and external fluids, respectively. When $D_f>0$, the filament tends to become a flat ribbon parallel to the electric field, while when $D_f<0$, the ribbon is deformed in a direction perpendicular to the field. Rhodes *et al.* performed experiments using an AC field instead of a DC field (for low enough frequency, the electrohydrodynamic flattening follows the same laws) and obtained good agreement with their theory.

The control of this electrohydrodynamic distortion is of great importance to the possible application of CFE. Recently, Heller *et al.*[8] have shown that the application of a second, oscillatory, electric field perpendicular to both the filament and to the first continuous field cancels this filament distortion, as each field leads to flattening in opposite directions, and we briefly recall their approach. Their experiment, closely inspired from that used in Ref. 5, was performed in a continuous flow electrophoresis apparatus, with a chamber $15\times6\times0.6$ cm (length-width-thickness). The thickness was deliberately chosen larger than in conventional CFE apparati and the multiple collection ports at the outlet end of the chamber were replaced by a window which allows direct observation of the section of the sample stream. A DC field was imposed along the width of the chamber using platinum electrodes and two dialysis membranes. The (length×width) sides of the chamber were made of two metal plates, covered with a thin (3 μm) continuous dielectric layer on the side in contact with the separation chamber. These metal plates were connected to a high frequency AC power supply operating at 50 kHz. The dielectric layers act as capacitors, and their impedance at 50 kHz is negligible as compared with that of the electrolyte solution, which allows application of a uniform AC field along the thickness of the chamber. The impedance with respect to the DC field is very high, however, so that the metal plates do not perturb the DC field acting along the width of the chamber.

When a sample stream with a conductivity higher than that of the separation buffer was introduced into the chamber, in the presence of the sole DC field, the sample filament distorted into a ribbon aligned parallel to the DC field (flattening in the opposite direction was observed for a sample less conductive than the electrolyte). This deformation was reduced when the AC field perpendicular to the DC field was applied and the sample stream width decreased with increasing AC field strength, until a circular shape was recovered. This optimal correction of sample filament shape occurred when the amplitude of the (sinusoidal) AC field was $\sqrt{2}$ times that of the DC field (within experimental error). When the AC field was increased beyond this value, the sample stream deformed in the other direction (i.e., along the thickness of the chamber). (For more details, see Ref. 8.)

In the present paper, we analyze theoretically the processes at play in this new experimental approach. In particular, we discuss the stability of the obtained equilibrium with respect to small elliptical perturbations of the cross section. We show that the circular cross section of the filament is stable when a new discriminating function $D_{f2}=(R-1)D_f$ is positive:

$$D_{f2}=(R-1)(R^2+R+1-3S)>0. \tag{2}$$

In the unstable case ($D_{f2}<0$), the efficiency of the separation process remains, however, substantially enhanced with respect to the single-field method developed by Rhodes *et al.*,[5] as the elliptical perturbations have to develop from an unstable equilibrium state, instead of simply evolving from a nonequilibrium initial configuration. So the basic, circular, filament configuration is in some sense more ''stable.'' A brief account of these theoretical results was given in Ref. 8 without the derivation from hydrodynamics that is supplied here.

In Sec. II, we recall the original single electric field results obtained by Rhodes *et al.*[5] for a circular filament, and we emphasize simple physical interpretations of the flattening effect based on a qualitative analysis of the forces applied on both sides of the interface. The forces are direct consequences of the appearance of free charges localized at the interface because of the conductivity contrast, and also of charge polarization associated with the permittivity contrast. Both electrical effects are therefore proportional to the square of the applied field. We show, as in our previous paper,[8] that the combination of two orthogonal electric fields $E_x=E_0$ and $E_y=E_1\cos(\omega t)$ allows the electrohydrodynamic distortion to be canceled, provided that:

$$E_1=\sqrt{2}E_0, \tag{3}$$

i.e., the mean square amplitude of the oscillatory field must be equal to the amplitude of the constant field (recall that the electrohydrodynamic effect is a quadratic function of the applied field). In Sec. III, these calculations are generalized to the two-field problem in the case of a slightly elliptic section. We show that this problem can be reduced to the flow calculations of Sec. II, with a modified stress distribution at the interface. The stability of the circular cross section is governed by the sign of the function D_{F2}. We then discuss in Sec. IV the applicability of these calculations to CFE. In general, the stability condition is not achieved in the usual experimental conditions, but even in the unstable case the efficiency of the separation remains enhanced by the application of the second field.

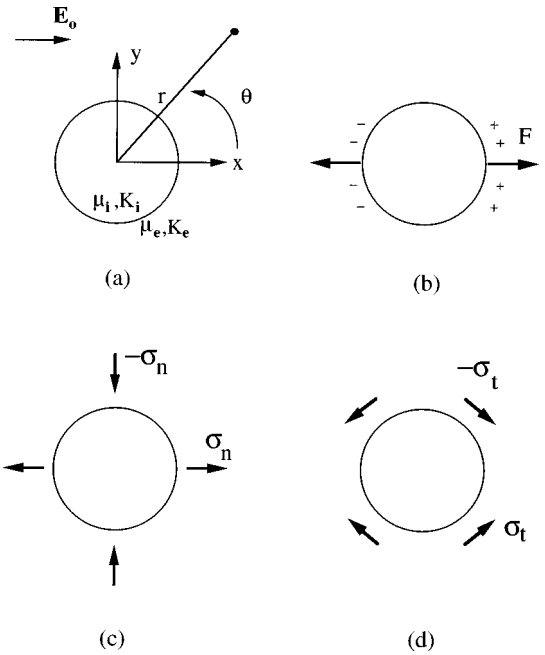

FIG. 2. (a) The application of a constant, uniform field on a cylindrical fluid inclusion would generate electric currents in both media that in turn induce a free charge distribution (b) at the interface (the case $\mu_i > \mu_e$ is suggested here). This charge distribution is submitted to stresses of electrical origin that should tend to flatten the fluid inclusion. (c) and (d): After removing an isotropic contribution, the previous stress distribution can be decomposed in two different elongation distributions (normal and shear components).

In all of their calculations, Rhodes *et al.*[5] used a sharp interface approximation in which the fluid properties change discontinuously from one bulk value to another. This idea had been introduced in a study of the similar problem of electric-field-induced deformations of spherical drops.[12] Saville recently suggested[9] that a more refined analysis involving a diffuse transition between the two fluids could lead to a modification of the predictions with respect to the influence of the permittivity ratio. However, this theory is still awaiting experimental confirmation and requires the introduction of an unknown concentration profile, and so for simplicity we have restricted our analysis to the sharp interface approximation. Several technical aspects of our calculations are detailed in the Appendixes, in which we also checked our results by comparing different solution methods. In the conclusion we discuss possible extensions of these calculations.

II. SINGLE FIELD AND TWO-FIELD PROBLEMS ON A CIRCULAR SECTION

The geometry of the problem is shown in Fig. 2(a). For simplicity, we neglect any three-dimensional effects (i.e., axial variations) and consider an idealized geometry in two dimensions: an infinite circular cylinder of electrolyte (conductivity μ_i, electrical permittivity K_i, radius a), is surrounded by another electrolyte (conductivity μ_e, electrical permittivity K_e), which extends to infinity. Both fluids are supposed to be initially at rest. We neglect any effects of interfacial tension and the possible diffusion of one fluid into the other. This system is suddenly submitted to an external uniform electric field (imposed at infinity) directed in the x-direction, $\mathbf{E}=E_0\mathbf{e}_x$ which is transverse to the flow direction. For completeness, we first recall and follow the argument developed by Rhodes *et al.*[5] The two-dimensional flow $\mathbf{u}(r,\theta)=(u_r,u_\theta)$ induced by electrohydrodynamics is calculated in order to predict the evolution of the cross sectional shape which leads to the flattening. We present a qualitative discussion of the physics involved in the simplest case $S=1$ and $R=\mu_i/\mu_e>1$ (filament lying inside a lower conductivity fluid, but with the same permittivity), and then develop the calculations in the general case $R\neq 1$ and $S\neq 1$.

A. A qualitative discussion of the case $S=1$ and $R>1$

When the field E_0 is applied to the system, electric currents are induced both inside the cylindrical inclusion $\mathbf{j}_\mathbf{x}^{(i)}=\mu_i E$, and in the external medium $\mathbf{j}_\mathbf{x}^{(e)}=\mu_e\mathbf{E}$. As $\mu_i\neq\mu_e$, the component of $\mathbf{j}$ normal to the interface is discontinuous and on a very short time scale surface charges accumulate at the interface. These surface charges, sketched in Fig. 2(b), induce an extra ''depolarizing'' field inside the inclusion in addition to an external dipole field, both fields allowing the system to recover the continuity of the normal electric current. However, the system will be now mechanically out of equilibrium, as the original electric field induces forces on these interfacial charges. Thus a distortion, or a ''flattening'' effect, is to be expected [see Fig. 2(b)]. The intensity of this effect is governed by a balance between the viscous hydrodynamic stresses and the electrical stresses transmitted to the liquid. In the case $R>1$, one would therefore expect a flattening of the section in the x-direction (i.e., parallel to the field). The same argument developed for the opposite case $(R<1)$ would lead to a transverse flattening in the y-direction (i.e., perpendicular to the field).

In fact the actual physical situation is more complicated, as the charge distribution also experiences its own induced field. In addition, $S\neq 1$ in general, and other forces associated with the permittivity contrast appear (polarization charges). Therefore the exact calculation of the flattening effect requires the use of the general formalism of electromagnetism for dielectric, conductive media[1,12] (i.e., calculation of the Maxwell stresses).

B. Electric field and electric potential

The calculation of the field associated with the presence of the cylindrical column is a classical problem of electromagnetism. One has to solve the Laplace equation for the potential $V(r,\theta)$:

$$\Delta V=0, \tag{4}$$

combined with the boundary conditions $V=-E_0x$ at infinity and the continuity of the normal electric current and the tangential component of the electric field at the interface $(r=a)$. Symmetry arguments suggest a solution of the form $V=f(r)\cos(\theta)$, and denoting the external and internal solutions, respectively, V_e^0 and V_i^0 (the superscript indicates that these potentials will serve later as the base state in the perturbation calculations developed in Sec. III), we find:

$$V_e^0=(aE_0)\left[-\frac{r}{a}+\left(\frac{R-1}{R+1}\right)\frac{a}{r}\right]\cos\theta \quad \text{for } r>a, \tag{5a}$$

$$V_i^0=-(aE_0)\,\frac{2}{R+1}\,\frac{r}{a}\cos\theta \quad \text{for } r<a, \tag{5b}$$

where R and S designate, respectively, the conductivity ratio $R=\mu_i/\mu_e$ and the permittivity ratio $S=K_i/K_e$. The radial and angular components of the associated electric fields are

$$(E_r)_e=E_0\left[1+\left(\frac{R-1}{R+1}\right)\frac{a^2}{r^2}\right]\cos\theta \quad \text{for } r>a, \tag{6a}$$

$$(E_\theta)_e=E_0\left[-1+\left(\frac{R-1}{R+1}\right)\frac{a^2}{r^2}\right]\sin\theta$$

and

$$(E_r)_i=\frac{2}{R+1}\,E_0\cos\theta \quad \text{for } r<a. \tag{6b}$$

$$(E_\theta)_i=-\frac{2}{R+1}\,E_0\sin\theta$$

The external potential is simply that of a dipole combined with the applied uniform field, while the internal field is uniform:

$$(E_X)_i=\frac{2}{R+1}\,E_0. \tag{7}$$

As usual, the external dipole field and the internal depolarizing field can be understood as the electric field induced by two distributions of surface charges localized at the interface: (1) the free charges q_s equal to the discontinuity of the normal component of the electric displacement field $\mathbf{D}=K\mathbf{E}$ and (2) the induced dipolar charges associated with the contrast in permittivity. It is important to note that because of the conductivity contrast, the free charge distribution is nonzero:

$$q_s=K_e(E_r)_e-K_i(E_r)_i=2K_e\left(\frac{R-S}{R+1}\right)E_0\cos\theta. \tag{8}$$

Physically, the dynamics of the interface analyzed by Rhodes *et al.*[5] corresponds to forces of electrical origin acting on these free charges, which in turn exert stresses that drive the fluid motion. As explained above, this description is strictly true only in the case $S=1$, which is in fact the situation most often encountered. When $S\neq 1$, the electrical forces exerted at the interface will be also partly of dipolar origin.

C. Flow calculation: Equations of motion

As assumed by Rhodes *et al.*,[5] the flow is governed by Stokes equations

$$\nabla\cdot\underline{\underline{\sigma}}=0, \tag{9a}$$

i.e., $\partial\sigma_{ij}/\partial x_j=0$, in which the components of the stress tensor $\underline{\underline{\sigma}}$ read:

$$\sigma_{ij}=(\sigma^v)_{ij}+(\sigma^{e1})_{ij}, \tag{9b}$$

$$(\sigma^v)_{ij}=\eta\left(\frac{\partial u_i}{\partial x_j}+\frac{\partial u_j}{\partial x_i}\right)-p\,\delta_{ij}, \tag{9c}$$

$$(\sigma^{e1})_{ij}=\frac{K}{4\pi}\left(E_iE_j-\frac{E^2}{2}\,\delta_{ij}\right), \tag{9d}$$

where $(\sigma^v)_{ij}$ and $(\sigma^{e1})_{ij}$ designate, respectively, the Newtonian (viscous) part of the stress tensor and the electric stress tensor. Also, $\mathbf{u}(r,\theta)$ designates the fluid velocity, p is the thermodynamic pressure, η is the viscosity (it is necessary to distinguish in general between the internal η_i and external η_e viscosities); we note that the effective pressure field that combines the usual pressure and terms of electrical origin is $p+K(E^2/8\pi)$, neglecting compressibility effects.[5] These equations express the ''equilibrium'' between viscous stresses and stresses of electrical origin. By combining them with the incompressibility condition $\nabla\cdot\mathbf{u}=0$ and the irrotationality of the electric field, one can show that in the absence of free charges in the bulk of the liquid, the flow obeys the following equations:

$$\nabla\cdot\mathbf{u}=0, \tag{10a}$$

$$\eta\nabla^2\mathbf{u}=\nabla p. \tag{10b}$$

Electrical effects are confined to the interface and appear in the boundary conditions. The problem thus reduces to the calculation of a classical Stokes flow (without any electrical effects) induced by forces localized at the interface. These forces are deduced from the continuity conditions, which for the (circular) base state are written at the interface $r=a$. Using the notation $[G]=G_e-G_i$, these conditions are

$$[\mathbf{u}]=\mathbf{u}^{(e)}-\mathbf{u}^{(i)}=\mathbf{0}, \tag{11a}$$

$$[(\sigma^v)_{rr}]+[(\sigma^{e1})_{rr}]=0, \tag{11b}$$

$$[(\sigma^v)_{r\theta}]+[(\sigma^{e1})_{r\theta}]=0. \tag{11c}$$

Using cylindrical coordinates, the stress equilibrium equation yields:

$$-[p]+\left[2\mu\,\frac{\partial u_r}{\partial r}\right]+\sigma_r=0, \tag{12a}$$

$$\left[\mu\left(\frac{1}{r}\,\frac{\partial u_r}{\partial\theta}+\frac{\partial u_\theta}{\partial r}\right)\right]+\sigma_\theta=0 \tag{12b}$$

in which the electrical surface forces can be put in the form:

$$\sigma_r=\left[\frac{K}{8\pi}\,(E_r^2-E_\theta^2)\right]=\sigma_0+\sigma_n\cos(2\theta), \tag{13a}$$

$$\sigma_\theta=\left[\frac{K}{4\pi}\,E_\theta E_r\right]=\sigma_t\sin(2\theta), \tag{13b}$$

with

$$\sigma_0=\frac{K_eE_0^2}{4\pi}\,\frac{R-1}{R+1}, \tag{13c}$$

$$\sigma_n=\frac{K_eE_0^2}{4\pi}\,\frac{R^2+1-2S}{(R+1)^2}, \tag{13d}$$

$$\sigma_t = -\frac{K_e E_0^2}{2\pi}\frac{R-S}{(R+1)^2}. \tag{13e}$$

These normal and tangential surface forces are sketched in Figs. 2(c) and 2(d) (after removing the isotropic contribution σ_0) based on the angular dependences (13). One can deduce from this figure that a flattening effect generally occurs and the sign of this effect depends on a competition between the normal and transverse stresses. In the case $S=1$, both effects are proportional to $R-1$, that is to the surface charge density and act in the same direction. Thus the flattening direction can be deduced without calculation of the flow: when $R>1$, the circular section will evolve to a ribbon shape in the x-direction while for $R<1$, the ribbon will be parallel to y. In the general case ($S\neq 1$), one has to calculate the flow field in order to determine the evolution of the shape.

D. Flow calculation: The stream function method

The method used by Rhodes *et al.*[5] involves a stream function $\psi(r,\theta)$ defined as:

$$u_r = -\frac{1}{r}\frac{\partial \psi}{\partial \theta}, \quad u_\theta = \frac{\partial \psi}{\partial r}. \tag{14}$$

The incompressibility condition (10a) is automatically satisfied, and Eq. (10b) implies that $\psi(r,\theta)$ satisfies the biharmonic equation:

$$\Delta^2 \psi = 0. \tag{15}$$

The symmetries involved in this problem and the θ dependence of the interfacial stresses [Eqs. (13)] suggest solutions $\psi(r,\theta)=f(r)\sin(2\theta)$. Assuming in addition that the velocity vanishes at infinity, and remains regular at $r=0$, leads to the solutions:

$$\psi_e(r,\theta) = \left(A\frac{a^2}{r^2}+B\right)\sin(2\theta) \quad \text{for } r>a, \tag{16a}$$

$$\psi_i(r,\theta) = \left(C\frac{r^2}{a^2}+D\frac{r^4}{a^4}\right)\sin(2\theta) \quad \text{for } r<a. \tag{16b}$$

Following Rhodes *et al.*,[5] the four integration constants A, B, C and D are obtained by writing the continuity conditions (11a) and (12), after calculating from (16a) and (16b) the fields $\mathbf{u}(r,\theta)$, $\sigma^v(r,\theta)$ and $p(r,\theta)$ [this last one by integrating Eq. (10b)]. We refer to their paper for more details, and give here the final equations satisfied by A, B, C and D:

$$0 = A+B-C-D, \tag{17a}$$

$$0 = A+C+2D, \tag{17b}$$

$$a^2\sigma_t + (\eta_e+\eta_i)(12A+4B) = 0, \tag{17c}$$

$$a^2\sigma_n + (\eta_e+\eta_i)(12A+8B) = 0. \tag{17d}$$

For A and B one obtains

$$A = \frac{a^2}{3}\frac{\sigma_n-2\sigma_t}{4(\eta_e+\eta_i)}, \quad B = \frac{a^2(\sigma_t-\sigma_n)}{4(\eta_e+\eta_i)}. \tag{17e}$$

One can then deduce the radial component of the velocity calculated at the interface ($r=a$):

$$u_r(r=a,\theta) = \frac{a}{6(\eta_e+\eta_i)}(2\sigma_n-\sigma_t)\cos(2\theta) \tag{18a}$$

with

$$2\sigma_n-\sigma_t = \frac{K_e E_0^2}{2\pi}\frac{(R^2+R+1-3S)}{(R+1)^2} = \frac{K_e E_0^2}{2\pi}\frac{D_F}{(R+1)^2}. \tag{18b}$$

As expected, a flattening of the filament section occurs, the direction of which depends on the sign of the discriminating function $D_f = R^2+R+1-3S$: when $D_f>0$, the filament tends to become a flat ribbon parallel to the electric field, while when $D_f<0$, the ribbon is perpendicular to the field.

E. Case of an oscillatory field

As discussed by Rhodes *et al.*, these results not only hold for a constant field but also for an oscillatory applied field $E_x = E_1\cos(\omega t)$, provided that the frequency is not too high compared to the typical rate associated with the charge relaxation (typically $\omega < 10^6$ Hz). The surface charges may then be treated within a quasi-static approximation, so that the electric potentials are

$$V_e^0(r,\theta) = -E_1\left(r-\frac{R-1}{R+1}\frac{a^2}{r}\right)\cos(\omega t)\cos\theta \quad \text{for } r>a, \tag{19a}$$

$$V_i^0(r,\theta) = \frac{-2rE_1}{R+1}\cos(\omega t)\cos\theta \quad \text{for } r<a. \tag{19b}$$

Rhodes *et al.* also suggested replacing E_0^2 by the mean square value $\langle E_x^2\rangle = (E_1^2)/2$ in (18b). Actually, this substitution should be considered carefully because the ''true'' stress equilibrium condition at the interface involves time-dependent terms varying as $\cos(\omega t)$ and $\cos(2\omega t)$ in addition to the mean square values of the stresses. These terms would induce, in turn, time-dependent flows superposed on the expected mean flow. However, as usual in problems involving oscillatory boundary conditions,[13] these flows should remain confined near the interface in a boundary layer of typical thickness $\lambda = (\eta/\rho\omega)^{1/2}$. For the usual experimental conditions, $\eta \approx 1$ cP, $\rho \approx 1$ g/cm^3 and $\omega \approx 10^3-10^5$ Hz, so that λ is of the order 1–10 μm and thus this effect has a negligible impact in the ''macroscopic'' dynamics of the interface. However, for very low frequencies, this boundary layer effect would have to be reconsidered.

F. Flattening cancellation with a second field

In the case of a constant field $E_x = E_0$, a possible method for control of the ribbon flattening effect has been suggested and tested experimentally by Heller *et al.*[8] The experimental method consists of applying a second oscillatory electric field in the transverse direction, $E_y = E_1\cos(\omega t)$, in order that the flattening induced by the two transverse fields compensate each other. The influence of the two-component field

studied here can easily be obtained by a simple extension of Rhodes *et al.*'s calculations (see Ref. 8) or by the following symmetry argument.

Since the electrical stresses are quadratic with respect to the field, $u_r(r=a)$ must be a quadratic function of E_0 and E_1. The cross term E_0E_1 must vanish because it is not compatible with the symmetries of the problem (not invariant by changing the sign of E_1). Moreover, these possible cross terms are proportional to $\cos(\omega t)$, so that they vanish when averaged over a cycle. Finally, the two other quadratic terms involving E_0 and E_1 must reduce to the results of Rhodes *et al.* when one of the fields vanishes. The only possibility that remains is

$$u_r(r=a)=\frac{a}{12\pi}\frac{K_e}{\eta_e+\eta_i}\left(E_0^2-\frac{E_1^2}{2}\right)\frac{D_F}{(R+1)^2}\cos(2\theta). \tag{20}$$

The sign change for E_1 results from the fact that $\cos(2\theta)$ has to be replaced by $\cos(2(\theta-\pi/2))$. For $E_1=\sqrt{2}E_0$, the interface distortion is canceled and the circular cross section becomes an equilibrium shape of the interface. An experimental check of (20) was carried by Heller *et al.*,[8] who demonstrated that this method of using of a second transverse applied electric field allows improved separation by continuous flow electrophoresis.

The cancellation of flattening can also be directly predicted from Eqs. (12) and (13), by calculating the new electrical stress distribution applied at the interface:

$$\sigma_r=2\sigma_0+\sigma_n\cos(2\theta)+\sigma_n\cos\left(2\left(\theta-\frac{\pi}{2}\right)\right)=2\sigma_0, \tag{21a}$$

$$\sigma_\theta=\sigma_1\sin(2\theta)+\sigma_t\sin\left(2\left(\theta-\frac{\pi}{2}\right)\right)=0. \tag{21b}$$

For $E_1=\sqrt{2}E_0$, the electrical forces reduce to an isotropic contribution, hence only affect the pressure jump across the interface, and thus no flattening should occur. It is, however, necessary to note that the internal pressure will differ from the external one, by a factor:

$$[p]=p_e-p_i=2\sigma_0=\frac{K_eE_0^2}{2\pi}\frac{R-1}{R+1}. \tag{22}$$

This modification to the pressure field will be important in the two-dimensional stability of the circular section discussed in the next section and for future calculations of possible three-dimensional instabilities.

III. TWO FIELD PROBLEM ON A PERTURBED CIRCULAR SECTION

We now discuss the stability of the equilibrium obtained in the case $E_1=\sqrt{2}E_0$, with respect to weak elliptical perturbations of the interface. As we shall see, the circular cross section can in fact be unstable with respect to small perturbations of the perimeter, and a flattening of the column can occur even with the two cross electric fields, but the time dependent shape changes occur on a comparatively long time scale. We begin with a simple qualitative argument explaining the mechanism of this instability in the case $S=1$, and we develop the exact calculation for the general case in the following sections. We should emphasize that in a time-averaged sense the effect of the two fields (one steady and the other time periodic) is to produce a base state with zero fluid velocity but with nonzero steady components of electrical stresses.

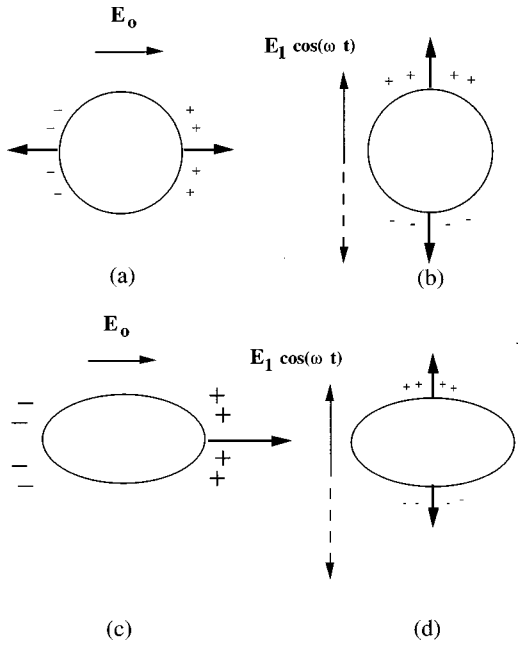

FIG. 3. (a) and (b): When two cross fields ($E_x=E_0$ and $E_y=E_1\cos\omega t$) are applied to a perfect cylindrical column, the stress associated to each charge distribution compensates each other when $E_1=\sqrt{2}E_0$. (c) and (d): When the section is initially slightly elliptic, the charge distribution lying near the largest curvature points is amplified. The resulting stress excess should tend to increase further the ellipticity of the fluid inclusion.

A. Instability under cross fields: A simple argument in the case $S=1$

The mechanism of the expected instability is suggested in Fig. 3. If two cross fields $E_x=E_0$ and $E_y=E_1\cos(\omega t)$ are applied to a circular inclusion, both fields will induce surface charges, but with different azimuthal distributions sketched in Figs. 3(a) and 3(b). Charges associated with E_0 are predominantly located near $\theta=0$ and $\theta=\pi$, while those induced by E_1 are near $\theta=\pm\pi/2$. As explained above, each charge distribution induces surface stresses that tend to induce two opposing shape changes. The equilibrium between these two effects is established for $E_1=\sqrt{2}E_0$.

If we suppose now that instead of being circular, the perimeter of the inclusion is initially slightly flattened, say in the x-direction [see Figs. 3(c) and 3(d)], the curvature of the surface will be larger near $\theta=0$ and $\theta=\pi$ than near $\theta=\pm\pi/2$. We therefore expect that the electric fields will be larger near $\theta=0$ and $\theta=\pi$, and that the first charge distribution (associated with E_0) will be amplified compared to the second one (associated with E_1). As a result, the distortion (flattening) induced by E_0 is expected to increase slightly and so exceed the distortion induced by E_1. The initial flattening perturbation of the circular cross section

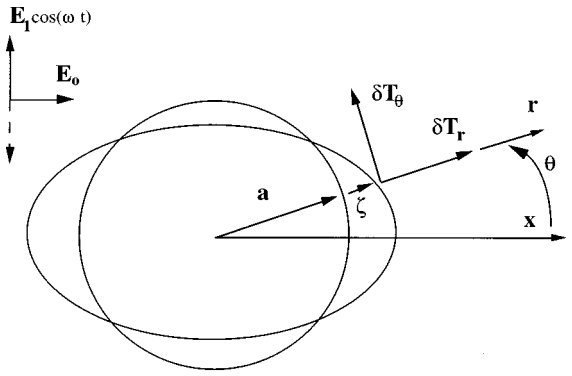

FIG. 4. Geometry of the stability calculations. The stresses δT_r and δT_θ must now be evaluated on a deformed interface, submitted to both translational and local rotational motions.

should therefore be amplified by a slight residual electrohydrodynamical flow. Intuitively, this argument is valid for $R>1$, as well as for $R<1$, and one may therefore expect that the circular cross section should be always unstable when $S=1$, except of course for the trivial case $R=1$.

Just as for the qualitative discussion of flattening with a single applied electric field discussed in Sec. II, the physical situation becomes more complicated when $S\neq 1$ because of the dipolar effects. As the single field flattening can be significantly affected by a permittivity contrast, we expect that stable equilibria exist for given values of R and S. We therefore present an exact calculation of the stability problem in the general case.

B. Electrical potentials for an elliptical cross section

Consistent with the azimuthal form of the electrical stresses acting at the interface [Eqs. (13)], we consider a slightly elliptical section described by the equation (see Fig. 4):

$$r=a[1+\epsilon(t)\zeta(\theta)]=a[1+\epsilon(t)\cos(2\theta)], \tag{23}$$

in which the ''eccentricity'' ϵ is a small parameter that measures small departures from the circular shape. At first order in ϵ, the application of the field E_0 leads to the appearance of the inner and outer electric potentials given by:

$$V_i=V_i^0(r,\theta)+\epsilon v_i(r,\theta) \quad \text{for } r<a, \tag{24a}$$

$$V_e=V_e^0(r,\theta)+\epsilon v_e(r,\theta) \quad \text{for } r>a, \tag{24b}$$

where V_i^0 and V_e^0 are the zeroth order potentials inside and outside, respectively, calculated in Sec. II B for a circular inclusion, while $v_i(r,\theta)$ and $v_e(r,\theta)$ are the perturbations (calculated at order ϵ) induced by the slight ellipticity of the cross section. v_e and v_i are calculated using the Laplace equation $\Delta v=0$, with the conditions that v_e is uniform at infinity and v_i is regular at $r=0$. In addition, the interface conditions are obtained by performing a Taylor series expansion about $r=a$:

$$v_e+a\zeta\frac{\partial V_e^0}{\partial r}=v_i+a\zeta\frac{\partial V_i^0}{\partial r} \quad \text{at } r=a, \tag{25a}$$

$$\mu_e\left\{\frac{\partial v_e}{\partial r}+a\zeta\frac{\partial^2 V_e^0}{\partial r^2}-\frac{\zeta'}{a}\frac{\partial V_e^0}{\partial\theta}\right\}=\mu_i\left\{\frac{\partial v_i}{\partial r}-\frac{\zeta'}{a}\frac{\partial V_i^0}{\partial\theta}\right\} \quad \text{at } r=a, \tag{25b}$$

where $\zeta'=\partial\zeta/\partial\theta$. The first condition (25a) ensures the continuity of the tangential component of the electric field, while the second condition (25b) expresses the continuity of the normal component of the electric current. Both conditions are written at order ϵ, the trivial condition at order ϵ^0 being subtracted (the calculation at order ϵ^0 leads to the ''unperturbed'' base potential given in Sec. II B). The symmetries of the problem suggest solutions of the form $f(r)\cos(\theta)+g(r)\cos(3\theta)$. After some calculations (see Appendix A) these solutions can be written as

$$v_e=aE_0\frac{R-1}{(R+1)^2}\left\{(R-1)\frac{a}{r}\cos\theta+(R+1)\frac{a^3}{r^3}\cos(3\theta)\right\}, \tag{26a}$$

$$v_i=-2aE_0\frac{R-1}{(R+1)^2}\frac{r}{a}\cos\theta \tag{26b}$$

for the perturbation of the electric potential, and

$$(\delta E_r)_e=\epsilon E_0\frac{R-1}{(R+1)^2}\left\{(R-1)\frac{a^2}{r^2}\cos\theta+3(R+1)\frac{a^4}{r^4}\cos(3\theta)\right\}, \tag{26c}$$

$$(\delta E_\theta)_e=\epsilon E_0\frac{R-1}{(R+1)^2}\left\{(R-1)\frac{a^2}{r^2}\sin\theta+3(R+1)\frac{a^4}{r^4}\cos(3\theta)\right\}, \tag{26d}$$

$$(\delta E_r)_i=2\epsilon E_0\frac{R-1}{(R+1)^2}\cos\theta, \tag{26e}$$

$$(\delta E_\theta)_i=-2\epsilon E_0\frac{R-1}{(R+1)^2}\sin\theta \tag{26f}$$

for the perturbations of the electric field. We note that the inner potential $V_i=V_i^0+\epsilon v_i$ still remains associated with a uniform electric field inside the inclusion, which could be expected because of the ellipsoidal shape of the interface.

The potential associated with the second oscillatory field could now be deduced very easily from that calculated for the first field. It is only necessary to replace E_0 with $E_1\cos(\omega t)$, ϵ with $-\epsilon$, and θ with $\theta-(\pi/2)$ in Eqs. (5) for the base potential and (26) for the perturbation. It will be simpler, however, in the next sections, to apply these symmetries to the electrical stresses rather than to the field, keeping in mind that the cross product terms (involving E_0 and E_1) vanish when averaged in time.

C. Electrical stresses on an elliptical cross section and induced hydrodynamic flow

The instantaneous hydrodynamic flow induced by the slight ellipticity of the cross section can be treated in the same spirit. One considers a velocity field $\mathbf{u}(r,\theta)$ and a pressure field given by:

$$\mathbf{u}(r,\theta)=\mathbf{0}+\delta\mathbf{u}(r,\theta), \tag{27a}$$

$$p(r,\theta)=p^0(r,\theta)+\delta p(r,\theta) \tag{27b}$$

in which we have distinguished an equilibrium base state (zero velocity, but nonuniform pressure field as $p_i^0 \neq p_e^0$), and two perturbation fields $\delta\mathbf{u}(r,\theta)$ and $\delta p(r,\theta)$ of order ϵ. These perturbation fields should again satisfy Stokes equation and the incompressibility condition in the bulk of both fluids:

$$\nabla\cdot\delta\mathbf{u}=0, \quad \eta\nabla^2\delta\mathbf{u}=\nabla\delta p. \tag{28}$$

Just as for the electric potential calculations, at first order in ϵ, the true ''jump'' conditions that should be written at the interface $(r=a(1+\epsilon\zeta))$ can be written at $r=a$:

$$[\delta\mathbf{u}]|_{r=a}=\delta\mathbf{u}_e-\delta\mathbf{u}_i=\mathbf{0}, \tag{29a}$$

$$[\delta\sigma_{rr}^v]|_{r=a}+\delta T_r=0, \tag{29b}$$

$$[\delta\sigma_{r\theta}^v]|_{r=a}+\delta T_\theta=0, \tag{29c}$$

where $\delta\sigma_{ij}^v$ designates the total Newtonian viscous stresses and $(\delta T_r,\delta T_\theta)$ are the perturbation stresses, which are all of electrical origin, including one term which enters owing to the base state having a (electrically produced) pressure jump across the interface. These stresses may be rewritten using a Taylor series about $r=a$ as

$$\delta T_r=[\delta\sigma_{rr}^{\mathrm{el}}]|_{r=a}+a\epsilon\zeta\left[\frac{\partial\sigma_{rr}^{\mathrm{el}(0)}}{\partial r}\right]\Bigg|_{r=a}-\epsilon\zeta'[\sigma_{r\theta}^{\mathrm{el}(0)}]|_{r=a}, \tag{30a}$$

$$\delta T_\theta=[\delta\sigma_{r\theta}^{\mathrm{el}}]|_{r=a}+a\epsilon\zeta\left[\frac{\partial\sigma_{r\theta}^{\mathrm{el}(0)}}{\partial r}\right]\Bigg|_{r=a}-\epsilon\zeta'[\sigma_{\theta\theta}^{\mathrm{el}(0)}]|_{r=a}-\epsilon[p^0]_{r=a}\zeta' \tag{30b}$$

in which $\sigma_{ij}^{\mathrm{el}(0)}$ designates the electrical stress associated with the base electric fields (calculated for the circular section), while $\delta\sigma_{ij}^{\mathrm{el}}$ designates the variation in electrical stresses induced by the perturbation of the field associated with the ellipticity. These stresses are

$$\sigma_{rr}^{\mathrm{el}(0)}=\frac{K}{8\pi}(E_r^2-E_\theta^2)=-\sigma_{\theta\theta}^{\mathrm{el}(0)}, \tag{31a}$$

$$\sigma_{r\theta}^{\mathrm{el}(0)}=\frac{K}{4\pi}E_rE_\theta, \tag{31b}$$

and

$$\delta\sigma_{rr}^{\mathrm{el}}=\frac{K}{4\pi}(E_r\delta E_r-E_\theta\delta E_\theta), \tag{32a}$$

$$\delta\sigma_{r\theta}^{\mathrm{el}}=\frac{K}{4\pi}(E_r\delta E_r+E_\theta\delta E_\theta), \tag{32b}$$

where here $E_r=-\partial V^0/\partial r$ and $E_\theta=-(1/r)\partial V^0/\partial\theta$ are the components of the base state electric field, while $\delta E_r=-\partial v/\partial r$ and $\delta E_\theta=-(1/r)\partial v/\partial\theta$ are the perturbation fields. The last term $[p^0]$ in Eq. (30b) represents the redistribution of the pressure stresses in the azimuthal direction due to the local inclination of the true normal to the surface $r=a$.

Using the expression of the potential calculated in Secs. II B and III B, we have calculated each term for the constant field E_0. As the cross terms $E_0E_1\cos(\omega t)$ vanish upon time averaging, we have then simply added to the result the averaged contribution arising from the second oscillatory field $E_1\cos(\omega t)$ deduced from the E_0 field by symmetry arguments. More precisely, any stresses can be calculated by the transformations: $E_0^2\to E_1^2/2=E_0^2$, $\epsilon\to-\epsilon$, $\theta\to\theta-\pi/2$. After some calculations (see Appendix B), the effective electrical stresses are found to be

$$\delta T_r=(\delta\sigma_n)\cos(2\theta), \tag{33a}$$

$$\delta T_\theta=(\delta\sigma_1)\sin(2\theta) \tag{33b}$$

with

$$\delta\sigma_n=\epsilon\frac{K_eE_0^2}{\pi}\frac{R-1}{(R+1)^3}(R^2+1-2S), \tag{34a}$$

$$\delta\sigma_t=-2\epsilon\frac{K_eE_0^2}{\pi}\frac{R-1}{(R+1)^3}(R-S). \tag{34b}$$

D. Flow calculation: Stability of the equilibrium

In order to evaluate the stability we again have, as in Sec. II, to solve a Stokes flow problem induced by surface stress distributions exhibiting the azimuthal dependence $\cos(2\theta)$ and $\sin(2\theta)$. The solution can be obtained without any more calculations, by simply using Eq. (18a) that relates the interface radial velocity to the effective electrical stress distribution. The radial velocity calculated at $r=a$ is simply given by

$$\delta u_r=\frac{a}{6(\mu_e+\mu_i)}(2\delta\sigma_n-\delta\sigma_t)\cos(2\theta) \tag{35a}$$

with

$$2\delta\sigma_n-\delta\sigma_t=\epsilon\frac{2K_eE_0^2}{\pi}\frac{R-1}{(R+1)^3}(R^2+R+1-3S). \tag{35b}$$

These results may be expressed as an evolution equation for the degree of ellipticity:

$$\frac{d\epsilon}{dt}=\frac{\epsilon}{\tau_0}\frac{R-1}{(R+1)^3}(R^2+R+1-3S) \tag{36a}$$

in which τ_0 is a typical time scale given by

$$\tau_0=3\pi\frac{\mu_e+\mu_i}{K_eE_0^2}. \tag{36b}$$

As discussed in the Introduction, we observe that the flattening stability of the circular cross section under cross electric fields depends on the new discriminating function

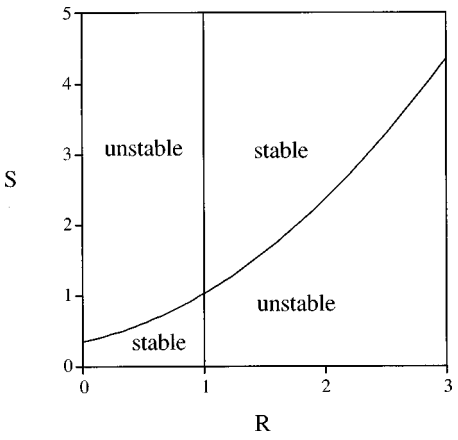

FIG. 5. Linear stability diagram obtained from our calculations ($R=\mu_i/\mu_e$ conductivity ratio, $S=K_i/K_e$ permittivity ratio).

$D_{f2}=(R-1)D_f=(R-1)(R^2+R+1-3S)$ introduced in Eq. (2). For $D_{f2}>0$, the circular cross section is unstable, while for $D_{f2}<0$, the circular shape is stable.

IV. DISCUSSION

We present in Fig. 5 the stability diagram in the (R,S) plane. Two stable ranges are observed and should be recommended for improvements of separation by continuous flow electrophoresis. Unfortunately, for the usual experimental conditions S is close to 1, and, as described in Sec. III A the circular filament is always unstable. It is, however, important to note that even for the unstable configuration, the separation remains greatly improved by the use of a secondary oscillatory field. This result may be verified by writing an equivalent of Eq. (36a) for the single field case, deduced from the results obtained in Sec. II:

$$\left(\frac{d\epsilon}{dt}\right)_{1\,\text{field}}=\frac{1}{4\tau_0}\,\frac{R^2+R+1-3S}{(R+1)^2}. \tag{37}$$

The ratio of the two growth rates is given by

$$\rho=\frac{(d\epsilon/dt)_{2\,\text{fields}}}{(d\epsilon/dt)_{1\,\text{field}}}=4\,\frac{R-1}{R+1}\,\epsilon_0, \tag{38}$$

where ϵ_0 is taken to be an order of magnitude of the possible flattening perturbations introduced at the chamber entrance by experimental imperfections. For representative values $R=4$ and $\epsilon=0.05$, one obtains a ratio of growth rates about 0.12, i.e., the filament deformation rate is reduced by an order of magnitude by the use of cross fields. This improvement comes from the fact that in the two-field case, the perturbations have to grow from an (unstable) equilibrium state, while in the single field case, the circular shape is an out-of-equilibrium configuration.

V. CONCLUSION

In summary, we have investigated the electrohydrodynamic flows induced by a single electric field or by two mutually perpendicular electric fields on a conductive column of electrolyte lying inside another electrolyte. In the single field case, the approach developed by Rhodes *et al.*[5] was summarized and we have given simple physical interpretations of the flattening of the filament cross section, which is due to electrical stresses that arise because of free charges in the immediate vicinity of the interface.

Furthermore, we have discussed the stability of the equilibrium obtained by the cross field technique proposed by Heller *et al.*,[8] which provides a possible method for control of the electrohydrodynamical distortions observed in free-flow electrophoresis. We have shown that the equilibrium is not always stable, and that the stability depends on the sign of a discriminating function involving the permitivity (S) and conductivity (R) ratios. For typical experimental conditions, the stable regions in the RS plane are not attained, though even in the unstable case, and by comparison with the single field case, the growth rate of filament distortion is reduced by the second electric field of optimized amplitude. The separation conditions are therefore expected to be improved by the addition of the second oscillatory field.

Various directions could now be explored. From an experimental point of view, the results obtained by Heller *et al.*[8] suggest a complete cancellation of the flattening effect and do not seem to reveal the ''flattening instability'' studied in Sec. III. This observation may be due to the range of flow velocities of the carrying fluid (the imposed Poiseuille flow in Fig. 1) studied in the experiment: the transit time of the charged species is reduced when the velocity is increased and the instability could require more time to be observed (exponential growth from very small perturbations). In practical situations, however, a better separation is presumably obtained when the flow rate is reduced in order to maximize the deflection of the charged particles. One can therefore not exclude the possible appearance of this instability in the future development of such cross-field techniques. In such a case, it would then be interesting to study the possible spatial dependence of the flattening effect in Heller *et al.*'s experiment by varying the flow rates in order to devise a simple criteria for the optimum velocity. From a more fundamental point of view, this spatial dependence may present some interesting connections with the absolute and convective instability criteria involved in open flows.[14]

Concerning the details of our calculations, it would certainly be interesting to extend the analysis to more complex perturbations of the filament shape, such as more general $\cos(n\theta)$ dependence of the filament perimeter. Unusual filament shapes (fourfold symmetries instead of the twofold one discussed in the present paper or highly nonlinear deformation of the section) are perhaps to be expected at very high fields.

Another possible direction would be the study of three-dimensional instabilities that could be related to the electrical pressure jump across the interface. Recent observations made by Sanchez and Clifton[15] show a breaking of the filament into droplets although capillary effects should not be involved (zero surface tension). On the other hand, similar observations were also reported by Kurowski and Petitjeans[16] on a liquid column flowing inside a miscible fluid without any electrical effect. The stability of such fluid columns in relation to the possible existence of weak effective transient surface tensions[17] is now under way.

A last improvement to be considered would be the replacement of the sharp interface assumed in the present paper by a more realistic diffuse interface. Such extensions of surface instabilities have been recently studied in the case of Saffman-Taylor instabilities or Rayleigh-Taylor instabilities.[18] Concerning the electrohydrodynamic effect in CFE, an attempt in this direction has been recently published by Saville[9] in the single field case, who suggests that the S dependence of the electrohydrodynamic effect could be modified. The extension of this study to the two-field case would be interesting.

ACKNOWLEDGMENTS

This work was initially motivated by a discussion with J. Prost. We thank M. Clifton and V. Sanchez for valuable discussions and for giving us recent information on the instability phenomena observed in CFE.

APPENDIX A: ELECTRIC POTENTIAL AND ELECTRIC FIELD CALCULATIONS

The electric potential $V(r,\theta)$ obeys the Laplace equation:

$$\frac{1}{r}\frac{\partial}{\partial r}\left(r\frac{\partial V}{\partial r}\right)+\frac{1}{r^2}\frac{\partial^2 V}{\partial \theta^2}=0. \tag{A1}$$

The solution for $r>a$ and $r<a$ can be developed over the cylindrical harmonics as

$$V_e=\left[-E_0 r+A_1\frac{a}{r}\right]\cos(\theta)+A_2\frac{a^2}{r^2}\cos(2\theta)+A_3\frac{a^3}{r^3}\cos(3\theta)+\cdots \quad \text{for } r>a, \tag{A2a}$$

$$V_e=B_1\frac{r}{a}\cos(\theta)+B_2\frac{r^2}{a^2}\cos(2\theta)+B_3\frac{r^3}{a^3}\cos(3\theta)+\cdots \quad \text{for } r<a. \tag{A2b}$$

The constants $\{A_i, B_i\}$ are given by the continuity conditions written for $r=a+\rho(\theta)$:

$$V_e(a+\rho,\theta)=V_i(a+\rho,\theta), \tag{A3a}$$

$$\mu_e\left[\frac{\partial V_e}{\partial r}-\frac{\rho'}{(a+\rho)^2}\frac{\partial V_e}{\partial \theta}\right]_{(r=a+\rho)}=\mu_i\left[\frac{\partial V_i}{\partial r}+\frac{\rho'}{(a+\rho)^2}\frac{\partial V_i}{\partial \theta}\right]_{(r=a+\rho)}. \tag{A3b}$$

For the unperturbed case ($\rho=0$), these conditions reduce to

$$-E_0 a+A_1=B_1, \quad -E_0 a-A_1=RB_1 \tag{A4}$$

or equivalently to

$$A_1=\frac{R-1}{R+1}E_0 a, \quad B_1=\frac{-2}{R+1}E_0 a, \tag{A5}$$

which lead to the potentials given in (5). In the perturbed case $\rho=\epsilon a\zeta(\theta)=\epsilon a\cos(2\theta)$, and at order ϵ, (A3) and (A4) reduce to (25). After eliminating the terms of order one, we find:

$$v_e-v_i=a\zeta[(E_r)_e-(E_r)_i]=(R-1)(E_r)_i a\zeta \quad \text{at } r=a, \tag{A6a}$$

$$\frac{\partial v_e}{\partial r}-R\frac{\partial v_i}{\partial r}=a\zeta\frac{\partial}{\partial r}(E_r)_e+(R-1)\zeta'(E_\theta)_i \quad \text{at } r=a, \tag{A6b}$$

in which E_r and E_θ designate the components of the zero order electric field (unperturbed potentials), the perturbations of the electric potential being, respectively, $\epsilon v_e(r,\theta)$ and $\epsilon v_i(r,\theta)$ outside and inside the inclusion. Using the expressions (6a) given in the text for E_r and E_θ, one can solve the problem seeking solutions:

$$v_e=\alpha_1\frac{a}{r}\cos(\theta)+\alpha_3\frac{a^3}{r^3}\cos(3\theta), \tag{A7a}$$

$$v_i=\beta_1\frac{r}{a}\cos(\theta)+\beta_3\frac{r^3}{a^3}\cos(3\theta). \tag{A7b}$$

Straightforward calculations give the constants α_1, α_2, β_1 and β_2:

$$\alpha_1-\beta_1=\alpha_3-\beta_3=\alpha_3+R\beta_3=-(\alpha_1+R\beta_1)=(aE_0)\frac{R-1}{R+1} \tag{A8}$$

which lead to

$$\alpha_1=(aE_0)\frac{(R-1)^2}{(R+1)^2}, \quad \beta_1=-2(aE_0)\frac{R-1}{(R+1)^2}, \tag{A9a}$$

$$\alpha_3=(aE_0)\frac{R-1}{R+1}, \quad \beta_3=0 \tag{A9b}$$

in agreement with the expressions (26) given in the text for the perturbed electric potentials.

APPENDIX B: CALCULATION OF THE ELECTRICAL STRESSES EXERTED ON THE PERTURBED INTERFACE

Each term involved in Eqs. (30), which give the normal and tangent component of the stress, has been first calculated from the field expressions given in Eqs. (6) and (26) for the continuous field $\mathbf{E}_0$. The results for the second field were then deduced from this first calculation by using the transformation $\{E_0^2\to E_1^2/2,\ \epsilon\to-\epsilon,\ \theta\to\theta-\pi/2\}$, and then added to the first result. For instance, the first term for the first field $\mathbf{E}_0$ is

$$[\delta\sigma_{rr}^{\mathrm{el}}]_{(E0)}=\epsilon\frac{K_e}{4\pi}E_0^2\frac{R-1}{(R+1)^3}\times\{R^2-1+4(R^2+R+1-S)\cos(2\theta)+3(R^2-1)\cos(4\theta)\}. \tag{B1}$$

As the cross terms vanish when averaged on one cycle, the E_1^2 contribution is

$$[\delta\sigma_{rr}^{\mathrm{el}}]_{(E1)}=(-\epsilon)\,\frac{K_e}{4\pi}\,\frac{E_1^2}{2}\,\frac{R-1}{(R+1)^3}\left\{R^2-1+4(R^2+R+1-S)\cos\left[2\left(\theta-\frac{\pi}{2}\right)\right]+3(R^2-1)\cos\left[4\left(\theta-\frac{\pi}{2}\right)\right]\right\}. \tag{B2}$$

For $E_1^2=2E_0^2$, one gets

$$[\delta\sigma_{rr}^{\mathrm{el}}]_{(E0+E1)}=2\,\frac{K_e}{\pi}\,\epsilon E_0^2\,\frac{R-1}{(R+1)^3}\times(R^2+R+1-S)\cos(2\theta). \tag{B3a}$$

The same method was applied to the other terms, leading at first order in the small eccentricity parameter ϵ to:

$$a\zeta\left[\frac{\partial\sigma_{rr}^{\mathrm{el}(0)}}{\partial r}\right]_{(E0+E1)}=-\frac{K_e}{\pi}\,\epsilon E_0^2\,\frac{R^2-1}{(R+1)^2}\cos(2\theta), \tag{B3b}$$

$$-\zeta'[\sigma_{r\theta}^{\mathrm{el}(0)}]_{(E0+E1)}=0, \tag{B3c}$$

$$[\delta\sigma_{r\theta}^{\mathrm{el}}]_{(E0+E1)}=2\,\frac{K_e}{\pi}\,\epsilon E_0^2\,\frac{R-1}{(R+1)^3}\times(R^2+R+1+S)\sin(2\theta), \tag{B3d}$$

$$a\zeta\left[\frac{\partial\sigma_{r\theta}^{\mathrm{el}(0)}}{\partial r}\right]_{(E0+E1)}=0, \tag{B3e}$$

$$\zeta'[\sigma_{\theta\theta}^{\mathrm{el}(0)}]=-\zeta'[\sigma_{rr}^{\mathrm{el}(0)}]=2\,\frac{K_e}{\pi}\,\epsilon E_0^2\,\frac{R-1}{R+1}\sin(2\theta), \tag{B3f}$$

$$[p^0]\zeta'=2\,\frac{K_e}{\pi}\,\epsilon E_0^2\,\frac{R-1}{R+1}\sin(2\theta). \tag{B3g}$$

The two last terms are equal because of the normal stress equilibrium under cross fields obtained for the unperturbed interface, which implies $[\sigma_{rr}^{\mathrm{el}(0)}]-[p^0]=0$. Combining the three nonzero contributions, one finally gets the results displayed in Eqs. (33) and (34).

APPENDIX C: CHECK OF ELECTRICAL STRESSES BY ELLIPTICAL COORDINATES

In view of the complexity of the calculations presented in the previous appendix, we have checked our results by a different method, using the elliptical coordinates θ and ϕ defined as

$$x=c\,\cosh(\phi)\cos(\theta),\quad y=c\,\sinh(\phi)\sin(\theta) \tag{C1}$$

in which c is related to the major axis $2a_{\max}=2a(1+\epsilon)$ and minor axis $2a_{\min}=2a(1-\epsilon)$, by the relationships:

$$a_{\max}=c\,\cosh(\phi_0),\quad a_{\min}=c\,\sinh(\phi_0). \tag{C2}$$

The elliptic interface is defined as $\phi=\phi_0$. Rhodes *et al.*[5] calculated the components of the electric field at the interface, for single field case $\mathbf{E}_0=E_0\mathbf{e}_x$ applied at infinity. These components are given by

$$(E_\phi)_e=R(E_\phi)_i=R\,\frac{E_0 c}{h}\,\frac{1+\tau}{R+\tau}\sinh(\phi_0)\cos(\theta),$$

$$(E_\theta)_e=(E_\theta)_i=-\frac{E_0 c}{h}\,\frac{1+\tau}{R+\tau}\cosh(\phi_0)\sin(\theta) \tag{C3}$$

$$\text{with}\quad h^2=c^2[\sinh^2(\phi_0)+\sin^2(\theta)]$$

in which $\tau=a_{\max}/a_{\min}\approx 1+2\epsilon$ is the aspect ratio ($\epsilon\ll 1$). We have used these expressions to calculate the normal and tangent components of the stresses, respectively, given by

$$[\sigma_{\phi\phi}^{\mathrm{el}}]=\frac{K_e}{16\pi}\,\frac{E_0^2c^2}{h^2}\,\frac{(1+\tau)^2}{(R+\tau)^2}\{(R^2-S)\sinh^2(\phi_0)-(1-S)\cosh^2(\phi_0)+[(R^2-S)\sinh^2(\phi_0)+(1-S)\cosh^2(\phi_0)]\cos(2\theta)\}, \tag{C4a}$$

$$[\sigma_{\theta\phi}^{\mathrm{el}}]=-\frac{K_e}{8\pi}\,\frac{E_0^2c^2}{h^2}\,\frac{(1+\tau)^2}{(R+\tau)^2}\times(R-S)\sinh(\phi_0)\cosh(\phi_0)\sin(2\theta). \tag{C4b}$$

One can eliminate the two variables c and ϕ_0 that can be expressed as functions of τ by the relationships:

$$\sinh(\phi_0)=\frac{1}{\sqrt{\tau^2-1}}\quad\text{and}\quad\frac{c^2}{h^2}=\frac{\tau^2-1}{1+(\tau^2-1)\sin^2(\theta)}. \tag{C5}$$

After replacing these quantities by these expressions in (C4a) and (C4b), one obtains the stresses as functions of the aspect ratio:

$$[\sigma_{\phi\phi}^{\mathrm{el}}]=\frac{K_e}{16\pi}\,E_0^2\,\frac{(1+\tau)^2}{(R+\tau)^2}\,\frac{1}{1+(\tau^2-1)\sin^2(\theta)}\{R^2-S-(1-S)\tau^2+[R^2-S+(1-S)\tau^2]\cos(2\theta)\}, \tag{C6a}$$

$$[\sigma_{\theta\phi}^{\mathrm{el}}]=-\frac{K_e}{8\pi}\,E_0^2\,\frac{(1+\tau)^2}{(R+\tau)^2}\,\frac{\tau}{1+(\tau^2-1)\sin^2(\theta)}\times(R-S)\sin(2\theta). \tag{C6b}$$

One can now develop these expressions at first order in ϵ, adding the contribution to the stresses induced by the second field. As for the calculations developed in the previous appendix, one can simply deduce this new contribution from the first one by using the transformations: $E_0^2\to E_1^2/2$, $\theta\to\theta-\pi/2$, $\epsilon\to-\epsilon$. Ultimately, one gets

$$[\sigma_{\phi\phi}^{\mathrm{el}}]=\frac{K_e}{\pi}\,\epsilon E_0^2\,\frac{R-1}{(R+1)^3}\,(R^2+1-2S)\cos(2\theta), \tag{C7a}$$

$$[\sigma_{\theta\phi}^{\mathrm{el}}]=-2\,\frac{K_e}{\pi}\,\epsilon E_0^2\,\frac{R-1}{(R+1)^3}\,(R-S)\sin(2\theta), \tag{C7b}$$

which coincides exactly with the stresses δT_r and δT_θ calculated with the method developed in the text and in Appendix B.

[1]J. R. Melcher, *Continuum Electromechanics* (MIT, Cambridge, MA, 1981).
[2]W. B. Russell, D. A. Saville, and W. R. Schowalter, *Colloidal Dispersions* (Cambridge University Press, Cambridge, England, 1989).
[3]P. D. Grossman and J. C. Colburn, *Capillary Electrophoresis: Theory and Practice* (Academic, San Diego, 1992).
[4]K. Hannig and H. G. Heidrich, ''The use of continuous preparative free-flow electrophoresis for dissociating cell fractions and isolation of membranous components,'' Methods Enzymol. **31**, 746 (1974).
[5]P. H. Rhodes, R. S. Snyder, and G. O. Roberts, ''Electrohydrodynamic distortion of sample streams in continuous flow electrophoresis,'' J. Colloid Interface Sci. **129**, 78 (1989).
[6]M. J. Clifton, N. Jouve, H. Roux de Balmann, and V. Sanchez, ''Conditions for purification of proteins by free-flow zone electrophoresis,'' Electrophoresis **11**, 913 (1990); M. J. Clifton, H. Roux de Balmann, and V. Sanchez, ''Electrohydrodynamic deformation of the sample stream in continuous-flow electrophoresis with an AC electric field,'' Can. J. Chem. Eng. **70**, 1055 (1992).
[7]P. H. Rhodes, R. S. Snyder, G. O. Roberts, and J. C. Baygents, ''Electrohydrodynamic effects in continuous flow electrophoresis,'' Appl. Theor. Electrophoresis **2–3**, 87 (1991).
[8]C. Heller, L. Limat, P. Sergot, and J. L. Viovy, ''Control of electrohydrodynamic distortion of sample streams in continuous flow electrophoresis using oscillating fields,'' Electrophoresis **14**, 1278 (1993); J. L. Viovy, unpublished technical note, 1991.
[9]D. A. Saville, ''Electrohydrodynamic deformation of a particulate stream by a transverse electric field,'' Phys. Rev. Lett. **71**, 2907 (1993).
[10]P. Mitchell, ''Self-electrophoretic locomotion in microorganisms: Bacterial flagella as giant ionophores,'' FEBS Lett. **28**, 1 (1972); P. E. Lammert, J. Prost, and R. Bruinsma, ''Ion drive for vesicles and cells,'' J. Theor. Biol. **178**, 387 (1996).
[11]A. Ajdari, ''Generation of transverse fluid currents and forces by an electric field: electro-osmosis on charge-modulated and undulated surfaces,'' Phys. Rev. E **53**, 4996 (1996).
[12]G. I. Taylor, ''Studies in electrohydrodynamics: I. The circulation produced in a drop by an electric field,'' Proc. R. Soc. London, Ser. A **291**, 159 (1966).
[13]G. K. Batchelor, *An Introduction to Fluid Dynamics* (Cambridge University Press, Cambridge, England, 1967), Chap. 4-3.
[14]P. Huerre and P. A. Monkewtiz, ''Local and global instabilities in spatially developing flows,'' Annu. Rev. Fluid Mech. **22**, 473 (1990).
[15]M. Clifton and V. Sanchez (private communication).
[16]P. Kurowski and P. Petitjeans, ''Immiscible fluids/miscible fluids: interesting similitudes,'' C. R. Acad. Sci., Ser. IIb: Mec., Phys., Chim., Astron. **325**, 587 (1997).
[17]P. Petitjeans, ''A surface tension for miscible fluids,'' C.R. Acad. Sci., Ser. IIb: Mec., Phys., Chim., Astron. **322**, 673 (1996).
[18]G. M. Homsy, ''Viscous fingering in porous media,'' Annu. Rev. Fluid Mech. **19**, 271 (1987); P. Kurowski, C. Misbah, and S. Tchourkine, ''Gravitational instability of a fictitious front during mixing of miscible fluids,'' Europhys. Lett. **29**, 309 (1995), and references therein.